Dynamic Instabilities of Simple Inelastic Structures Subjected to Earthquake Excitation

Christoph Adam and Clemens Jäger

Abstract The seismic collapse capacity of highly inelastic non-deteriorating single-degree-of-freedom (SDOF) systems, which are vulnerable to the destabilizing effect of gravity loads (P-delta effect), is evaluated. The collapse capacity based on different definitions of the intensity measure is discussed. In particular, collapse capacity spectra are derived utilizing sets of Incremental Dynamic Analyses (IDAs) involving 44 recorded ground motions.

1 Introduction

A main objective of earthquake engineering is to provide the structure with an adequate margin of safety against collapse [1]. Observations of collapsed buildings in severe earthquake events reveal that sidesway collapse is the main mode of structural collapse. Sidesway collapse can be a result of successive reduction of the load bearing capacity of structural components. In inelastic flexible structures gravity loads acting through lateral displacements amplify structural deformations and stress resultants (P-delta effect), and thus may be another source of sidesway collapse. In many realistic cases collapse is a consequence of combined action of both effects [1].

In this study the focus is on collapse of highly inelastic single-degree-of-freedom (SDOF) structures, which are vulnerable to the P-delta effect. A profound insight into the P-delta effect on the inelastic seismic response of structures is given e.g. by Bernal [2], and Ibarra and Krawinkler [3]. Asimakopoulos et al. [4] and Villaverde [5] provide an overview on studies dealing with collapse by dynamic instability

C. Adam · C. Jäger
Unit of Applied Mechanics, University of Innsbruck, 6020 Innsbruck, Austria
e-mail: christoph.adam@uibk.ac.at; clemens.jaeger@uibk.ac.at

H. Irschik et al. (eds.), *Advanced Dynamics and Model-Based Control of Structures and Machines*, DOI 10.1007/978-3-7091-0797-3_2,

in earthquake excited structures. Fundamental studies of the effect of gravity on inelastic SDOF systems subjected to earthquakes have been presented in Bernal [6] and MacRae [7]. Miranda and Akkar [8] present an empirical equation to estimate the minimum lateral strength up to which P-delta induced collapse of SDOF systems is prevented. In Adam et al. [9, 10] so-called collapse capacity spectra have been introduced for the assessment of the seismic collapse capacity of SDOF structures.

In the present paper emphasis is given on the collapse capacity. Collapse capacity spectra based on different definitions of the intensity measure are derived utilizing a set of 44 ordinary ground motion records. Results and conclusions of this study are valid only for non-deteriorating cyclic behavior, i.e. strength and stiffness degradation is not considered.

2 Framework and definitions

2.1 The P-delta effect in inelastic SDOF systems

In the following the effect of a gravity load on an SDOF oscillator with inelastic spring characteristics is demonstrated considering an inverted mathematical pendulum of length h as shown in Fig. 1a [9, 10]. An inelastic rotational spring with initial stiffness k_r supports the bottom of the rigid rod of the pendulum, and a rotational damper with parameter r_r models structural viscous damping. For small angles, $|\varphi| \ll 1$, the horizontal displacement x of the lumped mass m serves as the characteristic quantity of deformation. The gravity load P generates a shearing of the hysteretic force-displacement $(f - x)$ relationship. Characteristic displacements (such as the yield displacement x_y) of this relationship remain unchanged, whereas

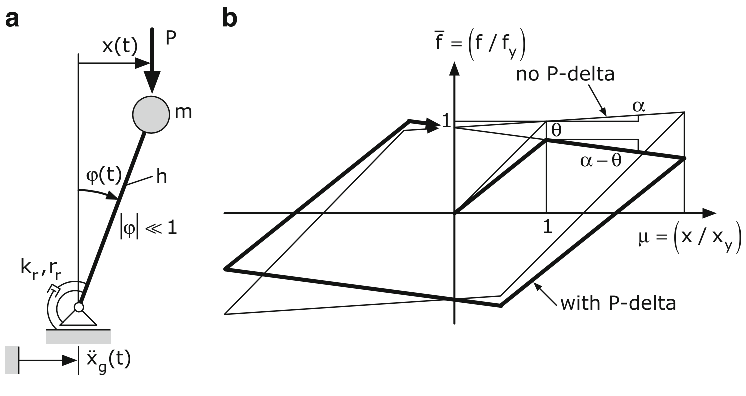

Fig. 1 (**a**) Mechanical model of the considered SDOF system. (**b**) Normalized bilinear cyclic behavior of the SDOF system with and without P-delta effect

the characteristic forces (such as the strength f_y) are reduced. The slope of the curve is decreased in its elastic and post-elastic branch of deformation. The magnitude of this reduction can be expressed by the stability coefficient [7, 10]:

$$\theta = \frac{Ph}{k_r} \tag{1}$$

As a showcase Fig. 1b visualizes the P-delta effect on the hysteretic behavior of an SDOF system with non-deteriorating bilinear characteristics. In this example the post-yield stiffness is negative because the stability coefficient θ is larger than the hardening ratio α.

A negative slope of the post-tangential stiffness, expressed by the difference of the stability coefficient θ and the strength hardening coefficient α, $\theta - \alpha$, is the essential condition that the structure may collapse under severe earthquake excitation. In [10] it is shown that collapse of inelastic SDOF systems vulnerable to P-delta is mainly governed by the following parameters:

- The negative slope of the post-tangential stiffness $\theta - \alpha$,
- the elastic structural period of vibration T,
- the viscous damping coefficient ζ (usually taken as 5%), and
- the shape of the hysteretic loop.

2.2 *Intensity measure and collapse capacity*

There is no unique definition of intensity of an earthquake record. Examples of the intensity measure are the 5% damped spectral acceleration S_a at the structure's period T, S_a $(T, \zeta = 0.05)$, the peak ground acceleration (PGA), the peak ground velocity (PGV), and the peak ground displacement (PGD), see e.g. [11]. An appropriate choice of the intensity measure exhibits a narrow distribution of deformation demands induced by a set of several earthquake records.

The collapse capacity is defined as the maximum ground motion intensity at which the structure still maintains dynamic stability [1]. The Incremental Dynamic Analysis (IDA) procedure [12] is applied to predict the collapse capacity. In an IDA for a given structure and a given acceleration time history of an earthquake record dynamic time history analyses are performed repeatedly, where in each subsequent run the intensity of the ground motion is incremented. As an outcome a characteristic intensity measure is plotted against the corresponding maximum characteristic structural response quantity for each analysis. The procedure is stopped, when the response grows to infinity, i.e. structural failure occurs. The corresponding intensity measure is referred to as collapse capacity of the considered structure for this specific ground motion record (denoted by i). In non-dimensional form the ith collapse capacity may be defined according to

$$CC|_{Sa(T),i} = \left.\frac{S_{a,i}(T)}{g\gamma}\right|_{collapse}, \quad CC|_{PGA,i} = \left.\frac{PGA_i}{g\gamma}\right|_{collapse}$$

$$CC|_{PGV,i} = \left.\frac{\omega\, PGV_i}{g\gamma}\right|_{collapse}, \quad CC|_{PGD,i} = \left.\frac{\omega^2\, PGD_i}{g\gamma}\right|_{collapse} \tag{2}$$

γ represents the yield strength coefficient, $\gamma = f_y/(mg)$, g is the acceleration of gravity, and ω denotes the structural circular frequency, $\omega = 2\pi/T$.

The inherent record-to-record variability leads to different collapse capacities for different ground motion records. Thus, the collapse capacities are determined for an entire set of n ground motion records, and subsequently evaluated statistically. For example, the median of the individual collapse capacities CC_i may be considered as representative collapse capacity CC for the analyzed structure and set of ground motion records. About 16% and 84% percentiles characterize the distribution of the individual collapse capacities.

As an example Fig. 2a shows IDA curves of an SDOF structure with bilinear hysteretic loop and the following structural parameters: $T = 1.0s$, $\zeta = 0.05$, $\theta - \alpha = 0.10$. In this example the intensity measure is the 5% damped spectral acceleration S_a at T. All results of this study are based on the ATC63 far-field (ATC63-FF) set of ordinary ground motions [13]. The records of this set originate from severe seismic events of moment magnitude between 6.5 and 7.6 and closest distance to the fault rupture larger than 10 km. Thereby, only strike-slip and reverse sources are considered. All 44 records of this set were recorded on NEHRP site classes C (soft rock) and D (stiff soil).

Different characteristics of the individual ground motion records lead to different IDA curves, which are plotted in grey, see Fig. 2a. A horizontal tangent of an IDA curve indicates structural failure. In this example the individual collapse capacities vary between 1.8 and 6.5. Furthermore, the median, 16% and 84% percentile curves are shown in black. Here, the intensity measure, where the median IDA curve becomes horizontally, is referred to as characteristic collapse capacity: $CC|_{Sa(T)} = 2.8$.

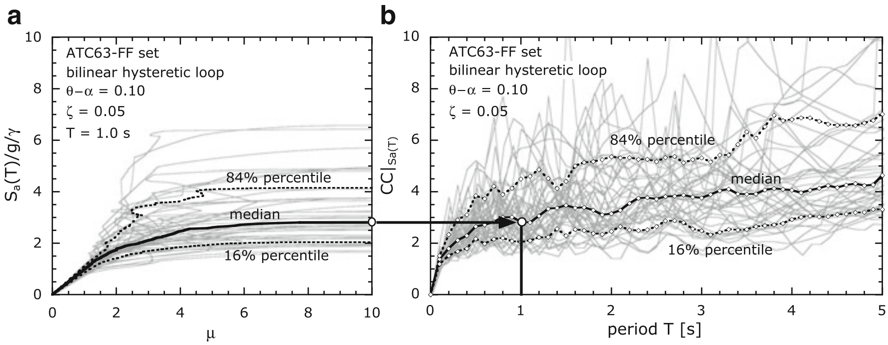

Fig. 2 (**a**) IDA curves, and (**b**) collapse capacity spectra. SDOF system, ATC63-FF set of ground motion records. Individual outcomes for each record and statistically evaluated results

3 Collapse capacity spectra

The representation of the collapse capacity of SDOF systems with assigned ζ and $\theta - \alpha$, and a particular hysteretic loop as a function of the initial period T results in collapse capacity spectra. Adam et al. [9, 10] introduce the concept of collapse capacity spectra for the assessment of the collapse capacity of non-deteriorating SDOF systems vulnerable to the P-delta effect. Exemplarily, Fig. 2b shows collapse capacity spectra of a bilinear SDOF system ($\zeta = 0.05$, $\theta - \alpha = 0.10$) for the 44 ground motions of the ATC63-FF set. Additionally, median, 16% and 84% percentile spectra are displayed in the period range between 0 and 5s.

Subsequently, collapse capacity spectra according to the definitions of (2) are compared and evaluated. Figure 3 reveals the different characteristics of median collapse capacity spectra exemplarily for SDOF systems with a negative post-yield slope of $\theta - \alpha = 0.06$ and a damping coefficient of $\zeta = 0.05$. Collapse capacities, which rely on PGA as intensity measure show a steep rise with increasing period. On the other hand, the graph of the median collapse capacity spectra based on S_a $(T, \zeta = 0.05)$ exhibits a decreasing gradient with increasing period. An appropriate intensity measure for a carefully selected set of ground motions leads to a narrow distribution of the individual collapse capacities. Figure 4 shows the characteristic quantity s of the distribution for the collapse capacity spectra presented in Fig. 3. Here, s is defined as the square root of the ratio of 84% percentile to 16% percentile collapse capacities,

$$s = \sqrt{\frac{CC|_{84\%}}{CC|_{16\%}}} \tag{3}$$

The larger the deviation of s from 1 the larger is the scatter of the individual results. From Fig. 4 it can be seen that s is for the collapse capacities based on the spectral

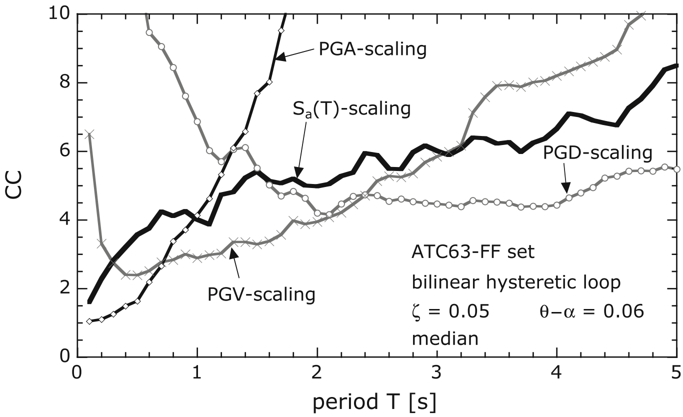

Fig. 3 Median collapse capacity spectra based on different definitions of the intensity measure

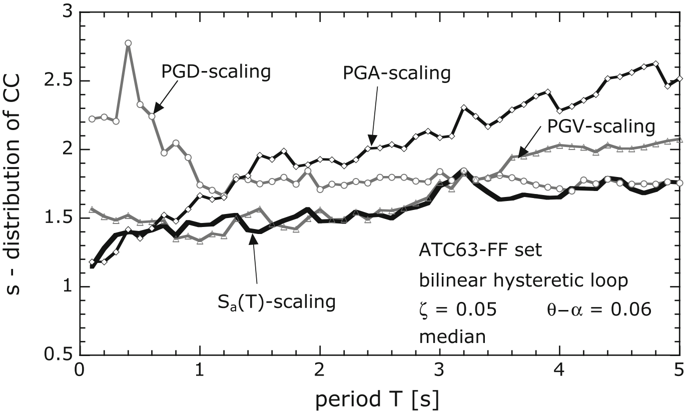

Fig. 4 Distribution of collapse capacity spectra based on different definitions of the intensity measure

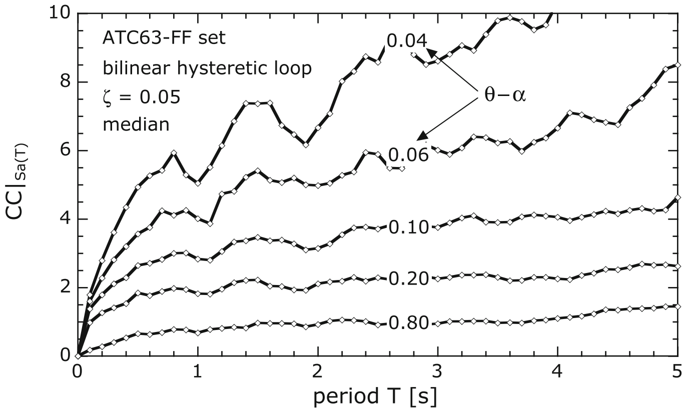

Fig. 5 Collapse capacity spectra based on the 5% damped spectral acceleration S_a at the structure's period T

acceleration a minimum in the nearly entire period range. For very stiff systems s is about 1.2 and then increases steadily with increasing period up to 1.75 at $T = 5.0s$. From this result it can be concluded that this definition of intensity measure is favorable for predicting the collapse capacity of SDOF structures vulnerable to P-delta. The other definitions of the intensity measures lead only at certain period segments to distributions comparable with S_a $(T, \zeta = 0.05)$. In the acceleration sensitive small period range PGA is an appropriate intensity measure, PGV in the velocity sensitive period range between 0.8 and 3.2s, and PGD leads in the large period range to a distribution similar to S_a $(T, \zeta = 0.05)$.

Figures 5–7 show collapse capacity spectra for a series of negative post-yield slopes $\theta - \alpha$ ranging from 0.04 to 0.80. The collapse capacities of these Figures

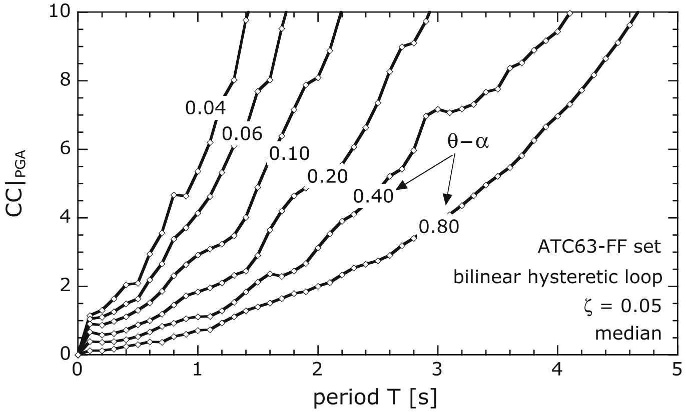

Fig. 6 Collapse capacity spectra based on the peak ground acceleration (PGA)

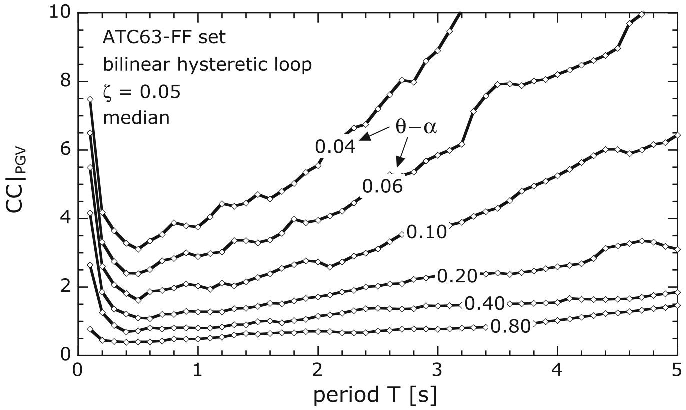

Fig. 7 Collapse capacity spectra based on the peak ground velocity (PGV)

rely on different definitions of the intensity measure: Fig. 5 is based on the 5% damped spectral acceleration S_a at the fundamental period T, Fig. 6 on PGA, and Fig. 7 on PGV. All representations have in common that an increasing slope of the negative stiffness reduces the collapse capacity. However, the run of the graphs is different for each definition, compare with Figs. 5–7. In particular, rigid systems ($T = 0$) exhibit for acceleration dependent intensity measures (i.e. $S_a(T)$ and PGA) a collapse capacity of $CC = 0$, whereas the application of PGV leads to a collapse capacity of infinity. This can be attributed to the fact that the definition of the PGV based collapse capacity is multiplied by the structure's fundamental frequency ω, which is infinity for $T = 0$, compare with (2).

Regression analyses convert collapse capacity spectra in design collapse capacity spectra with "smooth curves", compare with [10]. Application of design collapse capacity spectra is simple: an estimate of the elastic period of vibration T, stability coefficient θ and hardening ratio α of the actual SDOF structure need to be determined. Subsequently, from the chart the corresponding collapse capacity CC can be read [10].

In [14] it is shown that collapse capacity spectra can be applied to assess the collapse capacity of multi-degree-of-freedom (MDOF) systems vulnerable to P-delta, provided that a corresponding equivalent SDOF system reflects with sufficient accuracy the dynamic behavior of the MDOF system. In general, regular structures satisfy this requirement since the global P-delta effect is mainly governed by the fundamental mode. For further details see [14].

References

1. Krawinkler, H., Zareian, F., Lignos, D.G., Ibarra, L.F.: Prediction of collapse of structures under earthquake excitations. In: Papadrakakis M., Lagaros, N.D., Fragiadakis, M. (eds.) Proceedings of the 2nd International Conference on Computational Methods in Structural Dynamics and Earthquake Engineering (COMPDYN 2009), Rhodes, Greece, CD-ROM paper, paper no. CD449, 22–24 June 2009
2. Bernal, D.: Instability of buildings during seismic response. Eng. Struct. **20**, 496–502 (1998)
3. Ibarra, L.F., Krawinkler, H.: Global collapse of frame structures under seismic excitations. Report No. PEER 2005/06, Pacific Earthquake Engineering Research Center, University of California, Berkeley, CA, 2005
4. Asimakopoulos, A.V., Karabalis, D.L., Beskos, D.E.: Inclusion of the P-Δ effect in displacement-based seismic design of steel moment resisting frames. Earthquake Eng. Struct. Dyn. **36**, 2171–2188 (2007)
5. Villaverde, R.: Methods to assess the seismic collapse capacity of building structures: State of the art. J. Struct. Eng. **133**, 57–66 (2007)
6. Bernal, D.: Amplification factors for inelastic dynamic P-Δ effects in earthquake analysis. Earthquake Eng. Struct. Dyn. **15**, 635–651 (1987)
7. MacRae, G.A.: P-Δ effects on single-degree-of-freedom structures in earthquakes. Earthquake Spectra, **10**, 539–568 (1994)
8. Miranda, E., Akkar, S.D.: Dynamic instability of simple structural systems. J. Struct. Eng. **129**, 1722–1726 (2003)
9. Adam, C.: Global collapse capacity of earthquake excited multi-degree-of-freedom frame structures vulnerable to P-delta effects. In: Yang, Y.B. (ed.) Proceedings of the Taiwan – Austria Joint Workshop on Computational Mechanics of Materials and Structures, National Taiwan University, Taipei, Taiwan, pp. 10–13. 15–17 November 2008
10. Adam, C., Jäger, C.: Seismic collapse capacity of basic inelastic structures vulnerable to the P-delta effect, Earthquake Eng. Struct. Dyn. (accepted for publication)
11. Yakut, A., Yilmaz, H.: Correlation of deformation demands with ground motion intensity. J. Struct. Eng. **134**, 1818–1828 (2008)
12. Vamvatsikos, D., Cornell, C.A.: Incremental dynamic analysis. Earthquake Eng. Struct. Dyn. **31**, 491–514 (2002)
13. ATC63: Quantification of Building Seismic Performance Factors. Applied Technology Council ATC 63 Project Report – 90% Draft. FEMA P695, April 2008
14. Adam, C., Jäger, C.: Seismic induced global collapse of non-deteriorating frame structures. In: Papadrakakis, M., Lagaros, N.D., Fragiadakis, M. (eds.) Computational Methods in Earthquake Engineering, vol. 99, pp. 21–40. Springer, Dordrecht (2011)

Springer

http://www.springer.com/978-3-7091-0796-6

Advanced Dynamics and Model-Based Control of Structures and Machines
Irschik, H.; Krommer, M.; Belyaev, A.K. (Eds.)
2012, XIII, 241 p., Hardcover
ISBN: 978-3-7091-0796-6